CHAPTER EIGHT

Shells

In this chapter we consider thin composite shells, which we analyze on the basis of the main assumptions employed in the theory of thin plates. However, there is a major difference in the behavior of plates and shells subjected to external loads. Plates resist transverse loads by bending and by transverse shear forces. On the other hand, thin shells resist the transverse loads mostly by membrane forces, which, at any given point, are in the plane tangential to the reference surface (Fig. 8.1). These membrane forces are determined by the "membrane theory of shells," which neglects bending moments. The resulting stresses, strains, and deformations are reasonable except near supports and in the vicinities of abrupt changes in loads. For thick shells (whose thickness is comparable to the radii of curvature) or when regions near supports or concentrated loads are of interest, more complex analytical solutions or finite element methods must be employed. The decision as to which method to use rests with the individual and depends on his or her experience with analytical solutions and finite element calculations.

Herein we treat thin shells whose thickness h is small compared with all other dimensions and with the radii of curvatures (Fig. 8.2). The membrane forces N_x, N_y, N_{xy}, and N_{yx} acting at the reference surface of an infinitesimal element are[1]

$$\begin{aligned} N_x &= \int_{-h_b}^{h_t} \sigma_x \left(1 + \frac{z}{R_y}\right) dz \qquad N_y = \int_{-h_b}^{h_t} \sigma_y \left(1 + \frac{z}{R_x}\right) dz \\ N_{xy} &= \int_{-h_b}^{h_t} \tau_{xy} \left(1 + \frac{z}{R_y}\right) dz \qquad N_{yx} = \int_{-h_b}^{h_t} \tau_{yx} \left(1 + \frac{z}{R_x}\right) dz, \end{aligned} \tag{8.1}$$

where R_x and R_y are the radii of curvature in the x–z and y–z planes, and x, y, z are local coordinates with x and y in the plane tangential and z perpendicular to the reference surface at the point of interest (Fig. 8.2). The origin of the coordinate system is at the reference surface, which, conveniently, may be taken at the

[1] W. Flügge, *Stresses in Shells.* 2nd edition. Springer, Berlin, 1973, pp. 5–6.

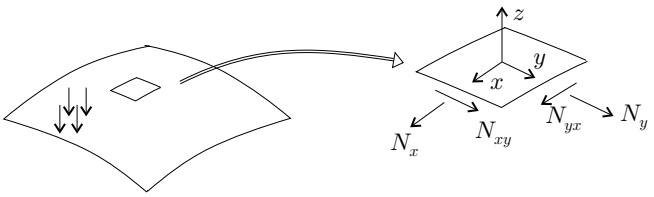

Figure 8.1: Membrane forces in a shell.

midsurface. For thin shells the quantities z/R_y and z/R_x are small with respect to unity, and these expressions reduce to

$$N_x = \int_{-h_b}^{h_t} \sigma_x dz \qquad N_y = \int_{-h_b}^{h_t} \sigma_y dz \qquad N_{xy} = N_{yx} = \int_{-h_b}^{h_t} \tau_{xy} dz. \tag{8.2}$$

In the "membrane theory of shells" the membrane forces depend only on the geometry, on the boundary conditions, and on the applied loads and are independent of the properties of the material. Hence, the membrane forces can be determined by the equations of static equilibrium.

The force–strain relationships are (Eq. 3.21)

$$\begin{Bmatrix} N_x \\ N_y \\ N_{xy} \\ M_x \\ M_y \\ M_{xy} \end{Bmatrix} = \begin{bmatrix} A_{11} & A_{12} & A_{16} & B_{11} & B_{12} & B_{16} \\ A_{12} & A_{22} & A_{26} & B_{12} & B_{22} & B_{26} \\ A_{16} & A_{26} & A_{66} & B_{16} & B_{26} & B_{66} \\ B_{11} & B_{12} & B_{16} & D_{11} & D_{12} & D_{16} \\ B_{12} & B_{22} & B_{26} & D_{12} & D_{22} & D_{26} \\ B_{16} & B_{26} & B_{66} & D_{16} & D_{26} & D_{66} \end{bmatrix} \begin{Bmatrix} \epsilon_x^o \\ \epsilon_y^o \\ \gamma_{xy}^o \\ \kappa_x \\ \kappa_y \\ \kappa_{xy} \end{Bmatrix}. \tag{8.3}$$

One of the major assumptions of the membrane theory is that changes in curvatures do not affect the stresses. With this assumption, from the preceding equation, the strains are

$$\begin{Bmatrix} \epsilon_x^o \\ \epsilon_y^o \\ \gamma_{xy}^o \end{Bmatrix} = \begin{bmatrix} A_{11} & A_{12} & A_{16} \\ A_{12} & A_{22} & A_{26} \\ A_{16} & A_{26} & A_{66} \end{bmatrix}^{-1} \begin{Bmatrix} N_x \\ N_y \\ N_{xy} \end{Bmatrix}, \tag{8.4}$$

where ϵ_x^o, ϵ_y^o, and γ_{xy}^o are the strains of the reference surface. This set of equations applies to symmetrical as well as to unsymmetrical layups even though the *form* of the equations is the same as for symmetrical laminates (Eq. 3.26). In the membrane

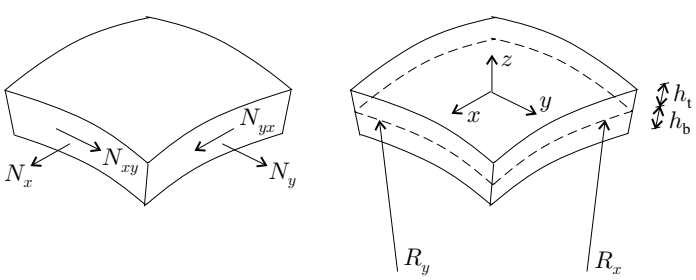

Figure 8.2: The membrane forces and the radii of curvatures of an element.

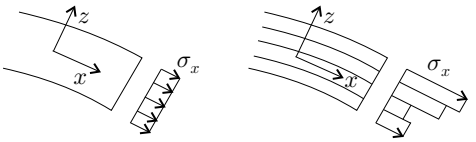

Figure 8.3: Stresses in an isotropic (left) and composite shell (right).

theory the strains are independent of the moments because the effects of changes in curvatures are neglected. In symmetrical laminates the strains are independent of the moments because the $[B]$ matrix is zero.

We neglect the variations of the strains across the thickness of the shell. Hence, the strains are

$$\begin{Bmatrix} \epsilon_x \\ \epsilon_y \\ \gamma_{xy} \end{Bmatrix} = \begin{Bmatrix} \epsilon_x^{\mathrm{o}} \\ \epsilon_y^{\mathrm{o}} \\ \gamma_{xy}^{\mathrm{o}} \end{Bmatrix}. \tag{8.5}$$

The stresses in each layer are then calculated by Eq. (2.126) as follows:

$$\begin{Bmatrix} \sigma_x \\ \sigma_y \\ \tau_{xy} \end{Bmatrix} = \begin{bmatrix} \overline{Q}_{11} & \overline{Q}_{12} & \overline{Q}_{16} \\ \overline{Q}_{12} & \overline{Q}_{22} & \overline{Q}_{26} \\ \overline{Q}_{16} & \overline{Q}_{26} & \overline{Q}_{66} \end{bmatrix} \begin{Bmatrix} \epsilon_x \\ \epsilon_y \\ \gamma_{xy} \end{Bmatrix}. \tag{8.6}$$

Note that the stress distributions differ in isotropic and composite shells. In an isotropic shell the stress distribution across the thickness is uniform, and the resultant of the stresses is in the midplane (Fig. 8.3). In a composite shell the stresses vary from layer to layer, and the resultant of the stresses generally is not in the midplane.

The stresses and strains resulting from the preceding analysis are used in the design of the membrane section.

Membrane forces for isotropic shells can be found in texts[2] and handbooks. These membrane forces also apply to composite shells. In the next section, we present results for thin composite shells of practical interest.

8.1 Shells of Revolution with Axisymmetrical Loading

A shell of revolution is obtained by rotating a curve, called the meridian, about an axis of revolution. We consider an element of the shell's reference surface formed by two adjacent meridians and two parallel circles (Fig. 8.4).

The load is axisymmetrical, and therefore there are no shear forces ($N_{xy} = 0$), and only N_x and N_y normal forces (per unit length) act. Force balance in the z direction (perpendicular to the surface) gives[3]

$$\frac{N_x}{R_x} + \frac{N_y}{R_y} = p_z, \tag{8.7}$$

where R_x is the radius of curvature of the meridian (Fig. 8.4) and R_y is along a line normal to the meridian with a length that is the distance between the reference

[2] Ibid.
[3] Ibid., p. 23.

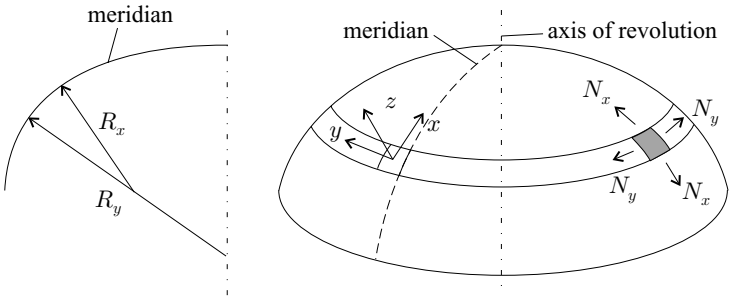

Figure 8.4: Shell of revolution.

surface and the point where the line intersects the axis of rotation; p_z is the component of the load normal to the surface at the point of interest (Fig. 8.5, left).

We now consider the portion of the shell above the parallel circle defined by ϕ (Fig. 8.5, right). We denote by F the resultant of all the loads acting on the shell above the parallel circle. A force balance along the axis of rotation gives

$$F + 2\pi r_0 N_x \sin\phi = 0, \tag{8.8}$$

where r_0 is defined in Figure 8.5. From the preceding equation, N_x is

$$N_x = -\frac{F}{2\pi r_0 \sin\phi}. \tag{8.9}$$

The forces N_y and N_x are calculated from Eqs. (8.7) and (8.9). Expressions for N_x and N_y are given in Table 8.1 for selected problems.

8.2 Cylindrical Shells

We consider thin-walled circular cylinders subjected to pressure p_z (which does not vary circumferentially), axial load $\widehat{N}$, and torque $\widehat{T}$ (Fig. 8.6).

8.2.1 Membrane Theory

By neglecting edge effects, one may calculate the membrane forces (Fig. 8.7) by the membrane theory. Force balances in the x and z directions and moment balance

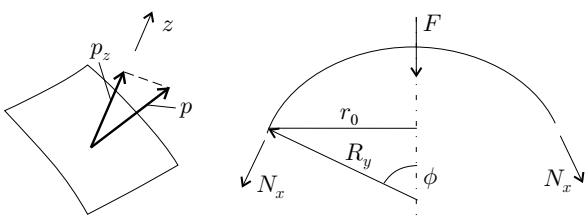

Figure 8.5: Load on an element and the free-body diagram for a shell of revolution.

Table 8.1. Membrane forces in spherical domes subjected to internal pressure (a), self-weight (b), and cones subjected to internal pressure (c); p, p_z, p_{z0} are in N/m^2; p_{z1} is in N/m^3.

(a)

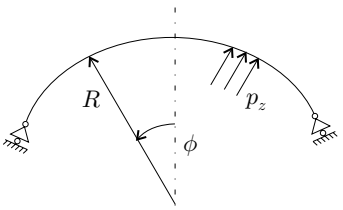

$$N_x = \tfrac{1}{2} p_z R$$
$$N_y = \tfrac{1}{2} p_z R$$

(b)

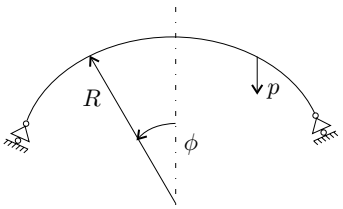

$$N_x = -\tfrac{pR}{1+\cos\phi}$$
$$N_y = pR\left(\tfrac{1}{1+\cos\phi} - \cos\phi\right)$$

(c)

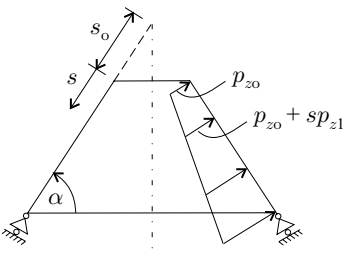

$$N_x = \tfrac{\cot\alpha}{s+s_o} s\left[p_{zo}\left(s_o + \tfrac{s}{2}\right) + p_{z1} s\left(\tfrac{s_o}{2} + \tfrac{s}{3}\right)\right]$$
$$N_y = \left(p_{zo} + sp_{z1}\right)(s + s_o)\cot\alpha$$

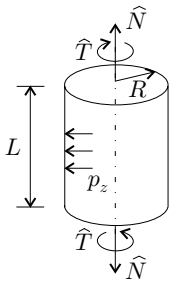

Figure 8.6: Thin cylinder subjected to radial pressure p_z (which does not vary circumferentially), axial load $\widehat{N}$, and torque $\widehat{T}$.

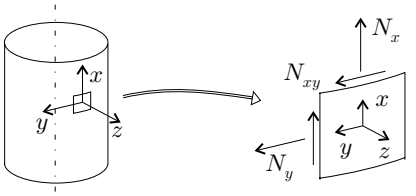

Figure 8.7: The membrane forces in a thin cylinder.

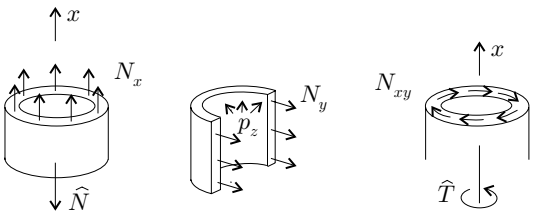

Figure 8.8: The loads and the membrane forces on a cylinder.

about the x-axis yield (Fig. 8.8)

$$\begin{aligned} N_x 2\pi R &= \widehat{N} \\ 2N_y &= p_z 2R \\ (N_{xy}R)\,2\pi R &= \widehat{T}, \end{aligned} \tag{8.10}$$

where R is the radius of the wall's reference surface. From these equations, the membrane forces are

$$N_x = \frac{\widehat{N}}{2\pi R} \qquad N_y = p_z R \qquad N_{xy} = \frac{\widehat{T}}{2\pi R^2}. \tag{8.11}$$

The strains corresponding to these membrane forces are calculated by Eq. (8.4). The axial u^{o}, radial w^{o}, and circumferential v^{o} displacements are

$$u^{\mathrm{o}} = \int \epsilon_x^{\mathrm{o}} dx = x\epsilon_x^{\mathrm{o}} + u_o^{\mathrm{o}} \qquad w^{\mathrm{o}} = R\epsilon_y^{\mathrm{o}} \qquad v^{\mathrm{o}} = \int \gamma_{xy}^{\mathrm{o}} dx = x\gamma_{xy}^{\mathrm{o}} + v_o^{\mathrm{o}}, \tag{8.12}$$

where u_o^{o} and v_o^{o} represent rigid-body motion.

8.2.2 Built-In Ends

As we noted previously, near boundary supports the membrane theory is inaccurate, and the forces, moments, and displacements of the shell must be calculated by other means. In the following, we consider thin-walled circular cylinders built-in at each end. The cylinder is subjected to pressure p_z, axial load $\widehat{N}$, and torque $\widehat{T}$

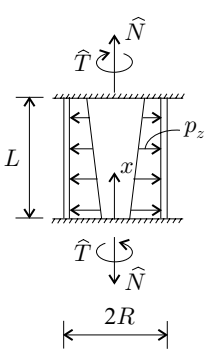

Figure 8.9: Cylinder built-in at both ends subjected to pressure p_z, axial load $\widehat{N}$, and torque $\widehat{T}$.

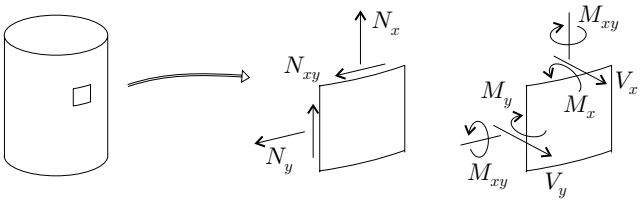

Figure 8.10: Forces and moments inside the wall of a thin cylinder.

(Fig. 8.9). The pressure may vary linearly along the cylinder's axis,

$$p_z = p_{z0} + x p_{z1}, \tag{8.13}$$

where p_{z0} and p_{z1} are specified constants. (For the pressure distribution shown in Fig. 8.9, p_{z1} is negative.) For the applied loads (Fig. 8.9), neither the stresses nor the strains vary circumferentially. Accordingly, the equilibrium equations are[4]

$$\frac{dN_x}{dx} = 0 \tag{8.14}$$

$$\frac{d}{dx}\left(RN_{xy} + M_{xy}\right) = 0 \tag{8.15}$$

$$\frac{N_y}{R} - \frac{d^2 M_x}{dx^2} = p_z \tag{8.16}$$

$$V_x = \frac{dM_x}{dx} \tag{8.17}$$

$$V_y = \frac{dM_{xy}}{dx}, \tag{8.18}$$

where the forces N_x, N_y, N_{xy}, the moments M_x, M_{xy}, and the transverse shear forces V_x and V_y are illustrated in Figure 8.10.

The strains and the curvatures of the reference surface are[5]

$$\epsilon_x^{\mathrm{o}} = \frac{du^{\mathrm{o}}}{dx} \qquad \epsilon_y^{\mathrm{o}} = \frac{w^{\mathrm{o}}}{R} \qquad \gamma_{xy}^{\mathrm{o}} = \frac{dv^{\mathrm{o}}}{dx} \tag{8.19}$$

$$\kappa_x = -\frac{d^2 w^{\mathrm{o}}}{dx^2} \qquad \kappa_y = -\frac{w^{\mathrm{o}}}{R^2} \qquad \kappa_{xy} = -\frac{2}{R}\frac{dv^{\mathrm{o}}}{dx}, \tag{8.20}$$

where u^{o}, v^{o}, and w^{o} are the axial, circumferential, and radial displacements of the reference surface.

The force–strain relationships are identical to those of laminated plates and are given by Eq. (8.3).

The equilibrium equations (Eqs. 8.14–8.18), the strain–displacement relationships (Eqs. 8.19–8.20), and the force–strain relationships (Eq. 8.3) provide the forces, moments, and displacements of the wall. In the following we reduce these equations to readily usable forms.

[4] Ibid., pp. 205–206.
[5] Ibid., p. 211.

Table 8.2. The parameters required in the equations

$$[a_1] = \begin{bmatrix} A_{22} - \frac{B_{22}}{R} & B_{12} \\ B_{12} - \frac{D_{12}}{R} & D_{11} \end{bmatrix} \qquad [a_3] = \begin{bmatrix} A_{11} & A_{16} - \frac{2B_{16}}{R} \\ A_{16} + \frac{B_{16}}{R} & A_{66} - \frac{B_{66}}{R} - \frac{2D_{66}}{R^2} \end{bmatrix}$$

$$[a_2] = \begin{bmatrix} A_{12} - \frac{B_{12}}{R} & B_{11} \\ A_{26} - \frac{D_{26}}{R^2} & B_{16} + \frac{D_{16}}{R} \end{bmatrix} \qquad [a_4] = \begin{bmatrix} A_{12} & A_{26} - \frac{2B_{26}}{R} \\ B_{11} & B_{16} - \frac{2D_{16}}{R} \end{bmatrix}$$

$$[H] = \begin{bmatrix} H_{11} & H_{12} \\ H_{21} & H_{22} \end{bmatrix} = [a_1] - [a_4][a_3]^{-1}[a_2]$$

$$\mathbf{g} = \begin{Bmatrix} g_1 \\ g_2 \end{Bmatrix} = [a_4][a_3]^{-1} \begin{Bmatrix} D_1 \\ D_2 \end{Bmatrix}$$

$$f_1 = H_{22} \quad f_2 = -\tfrac{1}{R}(H_{21} + H_{12}) \quad f_3 = \tfrac{H_{11}}{R^2} \quad f_4 = p_{z0} - \tfrac{g_1}{R} \quad f_5 = p_{z1}$$

The starting point of the analysis is the integration of the first two equilibrium equations (Eqs. 8.14 and 8.15). These integrations yield

$$\begin{aligned} D_1 &= N_x \\ D_2 &= N_{xy} + \frac{M_{xy}}{R}, \end{aligned} \tag{8.21}$$

where D_1, D_2 are as yet unknown constants. By substituting the force–strain relationships (Eq. 8.3) into Eq. (8.21) and by introducing Eqs. (8.19) and (8.20) into the resulting equations, we obtain

$$\begin{Bmatrix} D_1 \\ D_2 \end{Bmatrix} = [a_2] \begin{Bmatrix} \frac{w^o}{R} \\ -\frac{d^2 w^o}{dx^2} \end{Bmatrix} + [a_3] \begin{Bmatrix} \frac{du^o}{dx} \\ \frac{dv^o}{dx} \end{Bmatrix}. \tag{8.22}$$

The matrices $[a_2]$ and $[a_3]$ are given in Table 8.2.

From Eq. (8.22) the derivatives of u^o and v^o are

$$\begin{Bmatrix} \frac{du^o}{dx} \\ \frac{dv^o}{dx} \end{Bmatrix} = -[a_3]^{-1}[a_2] \begin{Bmatrix} \frac{w^o}{R} \\ -\frac{d^2 w^o}{dx^2} \end{Bmatrix} + [a_3]^{-1} \begin{Bmatrix} D_1 \\ D_2 \end{Bmatrix}. \tag{8.23}$$

The internal forces N_y and M_x may be expressed as (Eq. 8.3)

$$\begin{Bmatrix} N_y \\ M_x \end{Bmatrix} = \begin{bmatrix} A_{12} & A_{22} & A_{26} & B_{12} & B_{22} & B_{26} \\ B_{11} & B_{12} & B_{16} & D_{11} & D_{12} & D_{16} \end{bmatrix} \begin{Bmatrix} \epsilon_x^o \\ \epsilon_y^o \\ \gamma_{xy}^o \\ \kappa_x \\ \kappa_y \\ \kappa_{xy} \end{Bmatrix}. \tag{8.24}$$

By substituting Eqs. (8.19) and (8.20) into Eq. (8.24), we obtain

$$\begin{Bmatrix} N_y \\ M_x \end{Bmatrix} = [a_1] \begin{Bmatrix} \frac{w^o}{R} \\ -\frac{d^2 w^o}{dx^2} \end{Bmatrix} + [a_4] \begin{Bmatrix} \frac{du^o}{dx} \\ \frac{dv^o}{dx} \end{Bmatrix}. \tag{8.25}$$

The matrices $[a_1]$ and $[a_4]$ are given in Table 8.2. Substitution of Eq. (8.23) into Eq. (8.25) results in

$$\begin{Bmatrix} N_y \\ M_x \end{Bmatrix} = [H] \begin{Bmatrix} \frac{w^o}{R} \\ -\frac{d^2 w^o}{dx^2} \end{Bmatrix} + \begin{Bmatrix} g_1 \\ g_2 \end{Bmatrix}, \tag{8.26}$$

where $[H]$ and $\mathbf{g}$ are given in Table 8.2. This equation can be written as

$$N_y = H_{11} \frac{w^o}{R} - H_{12} \frac{d^2 w^o}{dx^2} + g_1 \tag{8.27}$$

$$M_x = H_{21} \frac{w^o}{R} - H_{22} \frac{d^2 w^o}{dx^2} + g_2, \tag{8.28}$$

where H_{11}, H_{12}, H_{21}, H_{22}, g_1, g_2 are the elements of the matrix $[H]$ and the vector $\mathbf{g}$. By introducing Eqs. (8.27) and (8.28) into the third equilibrium equation (Eq. 8.16) we obtain

$$f_1 \frac{d^4 w^o}{dx^4} + f_2 \frac{d^2 w^o}{dx^2} + f_3 w^o = f_4 + x f_5, \tag{8.29}$$

where $f_1, \ldots, f_5$ are given in Table 8.2. We note that f_4 contains the two as yet unknown constants D_1 and D_2.

Solution of this fourth-order differential equation yields the radial displacement of the reference surface[6]

$$\begin{aligned} w^o = \{ & e^{-\lambda x} [C_1 \cos(\beta x) + C_2 \sin(\beta x)] + e^{-\lambda(L-x)} [C_3 \cos(\beta(L-x)) \\ & + C_4 \sin(\beta(L-x))] \} + \left[\frac{1}{f_3} (f_4 + x f_5) \right], \end{aligned} \tag{8.30}$$

where L is the length of the cylinder and λ and β are the real and imaginary parts of the roots of the characteristic polynomial,

$$\begin{aligned} \lambda &= \mathrm{Re}(\gamma) \\ \beta &= \mathrm{Im}(\gamma) \end{aligned} \qquad \text{where} \quad \gamma = \sqrt{\frac{-f_2 + \sqrt{f_2^2 - 4 f_1 f_3}}{2 f_1}}. \tag{8.31}$$

Equation (8.30) is the solution of interest. This equation contains six unknown constants D_1, D_2, C_1–C_4. The constant D_1 is given by Eqs. (8.21) and (8.11)

$$D_1 = N_x = \frac{\widehat{N}}{2\pi R}. \tag{8.32}$$

The second equality in this equation is written by virtue of the fact that N_x is per unit length, $\widehat{N}$ is the total force, and $2\pi R$ is the circumference; D_2 is given by

[6] E. Kreyszig, *Advanced Engineering Mathematics*. 7th edition. John Wiley & Sons, New York, 1993, pp. 136–144.

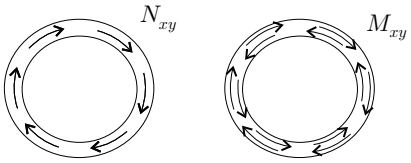

Figure 8.11: The shear force and the twist moment.

Eq. (8.21). The total torque acting at the edge of the cylinder is (Fig. 8.11)

$$\widehat{T} = (N_{xy} R)\, 2\pi R + M_{xy} 2\pi R. \tag{8.33}$$

Thus, from Eqs. (8.21) and (8.33) D_2 is

$$D_2 = \frac{\widehat{T}}{2\pi R^2}\cdot \tag{8.34}$$

The constants C_1–C_4 are obtained from the boundary conditions, which state that at a built-in end the radial displacement and its slope are zero as follows:

$$\begin{aligned} w^{\mathrm{o}} = 0 \quad \frac{dw^{\mathrm{o}}}{dx} = 0 \qquad \text{at} \quad x = 0 \\ w^{\mathrm{o}} = 0 \quad \frac{dw^{\mathrm{o}}}{dx} = 0 \qquad \text{at} \quad x = L. \end{aligned} \tag{8.35}$$

The derivative of w^{o} is given in Table 8.4. With the displacement given in Eq. (8.30), the boundary conditions above give

$$\begin{bmatrix} 1 & 0 & Y_{13} & Y_{14} \\ -\lambda & \beta & Y_{23} & Y_{24} \\ Y_{31} & Y_{32} & 1 & 0 \\ Y_{41} & Y_{42} & \lambda & \beta \end{bmatrix} \begin{Bmatrix} C_1 \\ C_2 \\ C_3 \\ C_4 \end{Bmatrix} = - \begin{Bmatrix} \frac{f_4}{f_3} \\ \frac{f_5}{f_3} \\ \frac{f_4 + L f_5}{f_3} \\ \frac{f_5}{f_3} \end{Bmatrix}, \tag{8.36}$$

where Y_{ij} are listed in Table 8.3. Equations (8.36) provide C_1–C_4. The displacement w^{o} is calculated with the constants D_1, D_2, C_1–C_4 thus determined.

Table 8.3. The parameters in Eq. (8.36)

$Y_{13} = e^{-\lambda L}\cos\beta L$	$Y_{14} = e^{-\lambda L}\sin\beta L$
$Y_{23} = e^{-\lambda L}(\lambda\cos\beta L + \beta\sin\beta L)$	$Y_{24} = e^{-\lambda L}(-\beta\cos\beta L + \lambda\sin\beta L)$
$Y_{31} = e^{-\lambda L}\cos\beta L$	$Y_{32} = e^{-\lambda L}\sin\beta L$
$Y_{41} = -e^{-\lambda L}(\lambda\cos\beta L + \beta\sin\beta L)$	$Y_{42} = e^{-\lambda L}(\beta\cos\beta L - \lambda\sin\beta L)$

Table 8.4. Displacement w^o of a cylinder, its derivatives, and its integral

$$
\begin{aligned}
w^o &= \tfrac{1}{f_3}(f_4 + x f_5) \\
&\quad + e^{-\lambda x}\cos(\beta x)C_1 \\
&\quad + e^{-\lambda x}\sin(\beta x)C_2 \\
&\quad + e^{-\lambda(L-x)}\cos(\beta(L-x))C_3 \\
&\quad + e^{-\lambda(L-x)}\sin(\beta(L-x))C_4
\end{aligned}
$$

$$
\begin{aligned}
\frac{dw^o}{dx} &= \tfrac{f_5}{f_3} + e^{-\lambda x}\cos(\beta x)(-\lambda C_1 + \beta C_2) \\
&\quad + e^{-\lambda x}\sin(\beta x)(-\beta C_1 - \lambda C_2) \\
&\quad + e^{-\lambda(L-x)}\cos(\beta(L-x))(\lambda C_3 - \beta C_4) \\
&\quad + e^{-\lambda(L-x)}\sin(\beta(L-x))(\beta C_3 + \lambda C_4)
\end{aligned}
$$

$$
\begin{aligned}
\frac{d^2w^o}{dx^2} &= e^{-\lambda x}\cos(\beta x)((\lambda^2-\beta^2)C_1 - 2\lambda\beta C_2) \\
&\quad + e^{-\lambda x}\sin(\beta x)(2\lambda\beta C_1 + (\lambda^2-\beta^2)C_2) \\
&\quad + e^{-\lambda(L-x)}\cos(\beta(L-x))((\lambda^2-\beta^2)C_3 - 2\lambda\beta C_4) \\
&\quad + e^{-\lambda(L-x)}\sin(\beta(L-x))(2\lambda\beta C_3 + (\lambda^2-\beta^2)C_4)
\end{aligned}
$$

$$
\begin{aligned}
\frac{d^3w}{dx^3} &= e^{-\lambda x}\cos(\beta x)(\lambda(3\beta^2-\lambda^2)C_1 + \beta(3\lambda^2-\beta^2)C_2) \\
&\quad + e^{-\lambda x}\sin(\beta x)(-\beta(3\lambda^2-\beta^2)C_1 + \lambda(3\beta^2-\lambda^2)C_2) \\
&\quad + e^{-\lambda(L-x)}\cos(\beta(L-x))(-\lambda(3\beta^2-\lambda^2)C_3 - \beta(3\lambda^2-\beta^2)C_4) \\
&\quad + e^{-\lambda(L-x)}\sin(\beta(L-x))(\beta(3\lambda^2-\beta^2)C_3 - \lambda(3\beta^2-\lambda^2)C_4)
\end{aligned}
$$

$$
\begin{aligned}
\int w^o dx &= \tfrac{1}{f_3}\left(f_4 x + \tfrac{x^2}{2} f_5\right) \\
&\quad + e^{-\lambda x}\cos(\beta x)\tfrac{-\lambda C_1 - \beta C_2}{\lambda^2+\beta^2} \\
&\quad + e^{-\lambda x}\sin(\beta x)\tfrac{\beta C_1 - \lambda C_2}{\lambda^2+\beta^2} \\
&\quad + e^{-\lambda(L-x)}\cos(\beta(L-x))\tfrac{\lambda C_3 + \beta C_4}{\lambda^2+\beta^2} \\
&\quad + e^{-\lambda(L-x)}\sin(\beta(L-x))\tfrac{-\beta C_3 + \lambda C_4}{\lambda^2+\beta^2}
\end{aligned}
$$

The expressions for the axial and circumferential displacements are obtained by integrating Eq. (8.23)

$$
\begin{Bmatrix} u^o \\ v^o \end{Bmatrix} = -[a_3]^{-1}[a_2]\begin{Bmatrix} \frac{\int w^o dx}{R} \\ -\frac{dw^o}{dx} \end{Bmatrix} + x\,[a_3]^{-1}\begin{Bmatrix} D_1 \\ D_2 \end{Bmatrix} + \begin{Bmatrix} u_o^o \\ v_o^o \end{Bmatrix}. \tag{8.37}
$$

The integral of w^o is included in Table 8.4, and u_o^o, v_o^o are rigid-body motions.

Once the displacements are known, all other parameters of interest can be calculated. The strains are calculated by Eqs. (8.19) and (8.20). (The derivatives appearing in these equations are listed in Table 8.4.) The forces and moments per unit length are calculated by Eq. (8.3).

Orthotropic cylinders. For orthotropic cylinders, $A_{16} = A_{26} = B_{16} = B_{26} = D_{16} = D_{26} = 0$, and the parameters in Table 8.2 become simpler, as shown in Table 8.5. With these parameters the radial displacement is given by Eq. (8.30),

Table 8.5. The parameters required in the equations for orthotropic cylinders

$$[a_1] = \begin{bmatrix} A_{22} - \frac{B_{22}}{R} & B_{12} \\ B_{12} - \frac{D_{12}}{R} & D_{11} \end{bmatrix} \qquad [a_3] = \begin{bmatrix} A_{11} & 0 \\ 0 & A_{66} - \frac{B_{66}}{R} - \frac{2D_{66}}{R^2} \end{bmatrix}$$

$$[a_2] = \begin{bmatrix} A_{12} - \frac{B_{12}}{R} & B_{11} \\ 0 & 0 \end{bmatrix} \qquad [a_4] = \begin{bmatrix} A_{12} & 0 \\ B_{11} & 0 \end{bmatrix}$$

$$[H] = \begin{bmatrix} H_{11} & H_{12} \\ H_{21} & H_{22} \end{bmatrix} = [a_1] - [a_4][a_3]^{-1}[a_2]$$

$$\mathbf{g} = \begin{Bmatrix} g_1 \\ g_2 \end{Bmatrix} = [a_4][a_3]^{-1} \begin{Bmatrix} D_1 \\ D_2 \end{Bmatrix}$$

$$f_1 = H_{22} \quad f_2 = -\tfrac{1}{R}(H_{21} + H_{12}) \quad f_3 = \tfrac{H_{11}}{R^2} \quad f_4 = p_{z0} - \tfrac{g_1}{R} \quad f_5 = p_{z1}$$

and the axial and circumferential displacements become

$$u^{\mathrm{o}} = \frac{1}{A_{11}} \left[- \left(A_{12} - \frac{B_{12}}{R} \right) \frac{\int w^{\mathrm{o}} dx}{R} + B_{11} \frac{dw^{\mathrm{o}}}{dx} + x D_1 \right] + u_o^{\mathrm{o}} \tag{8.38}$$

$$v^{\mathrm{o}} = \frac{x}{A_{66} - \frac{B_{66}}{R} - \frac{2D_{66}}{R^2}} D_2 + v_o^{\mathrm{o}}. \tag{8.39}$$

A detailed examination of Eq. (8.37) shows that cylinders with arbitrary layup rotate ($v^{\mathrm{o}} \neq 0$) when subjected to an axial load (Fig. 8.12). On the other hand, orthotropic cylinders do not rotate ($v^{\mathrm{o}} = 0$; see Eq. 8.39) when only an axial load acts.

End effects. We can see from Eq. (8.30) that the effects of the ends are confined to a narrow "boundary layer" and decay exponentially with λx. For example, within a distance $x = 4/\lambda$ from the end, the value of w^{o} is within 2 percent of the value given by the membrane theory.

For long cylinders the boundary layers extending from each end do not meet (Fig. 8.13) and there is a central region, which may be treated as a membrane. In this membrane region Eq. (8.30) reduces to

$$w^{\mathrm{o}} = \left\{ \frac{1}{f_3} (f_4 + x f_5) \right\} \qquad L_{\mathrm{B}} < x < L - L_{\mathrm{B}}. \tag{8.40}$$

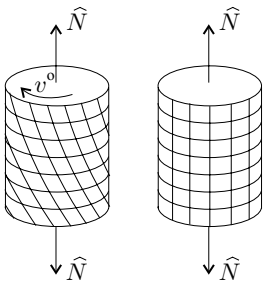

Figure 8.12: Cylinder subjected to axial load. Arbitrary layup (left); orthotropic layup (right).

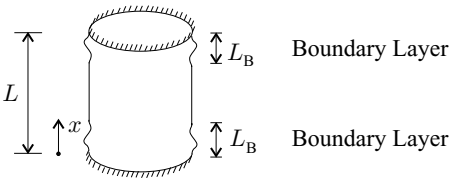

Figure 8.13: Illustration of the boundary layers.

When the two boundary layers do not interact, the support at $x = 0$ does not affect the boundary at $x = L$, and vice versa. Now, Eq. (8.30) becomes simpler, and within each boundary layer the radial displacement is given by

$$w^{\mathrm{o}} = e^{-\lambda x}[C_1 \cos(\beta x) + C_2 \sin(\beta x)] + \left[\frac{1}{f_3}(f_4 + x f_5)\right] \qquad 0 < x < L_{\mathrm{B}} \quad (8.41)$$

$$w^{\mathrm{o}} = e^{-\lambda (L-x)}[C_3 \cos \beta(L-x) + C_4 \sin \beta(L-x)] + \left[\frac{1}{f_3}(f_4 + x f_5)\right] \qquad L - L_{\mathrm{B}} < x < L, \quad (8.42)$$

where L_{B} is the length of the boundary layer (say, $L_{\mathrm{B}} = 4/\lambda$). When the length of the cylinder is $L > 2L_{\mathrm{B}}$, the boundary layers extending from the two ends do not meet. For $L_{\mathrm{B}} = 4/\lambda$, this gives $L > 8/\lambda$ or $\lambda L > 8$. When $\lambda L > 8$, the parameters Y_{ij} (Table 8.3) are negligible, and the constants C_1 and C_2 are determined from the first two rows, and C_3 and C_4 from the second two rows of Eq. (8.36).

8.1 Example. *An $L = 0.5$-m-long cylinder (inner radius $R_{in} = 0.2$ m) is made of graphite epoxy unidirectional plies. The material properties are given in Table 3.6 (page 81). The layup is $[0_{10}/45_{10}]$. The 0-degree plies are on the inside and are parallel to the cylinder's axis. The thickness of the wall is $h = 0.002$ m. The cylinder is built-in at both ends (Fig. 8.14). An axial load $\widehat{N} = 20\,000$ N is applied to the cylinder. Calculate the displacements along the length.*

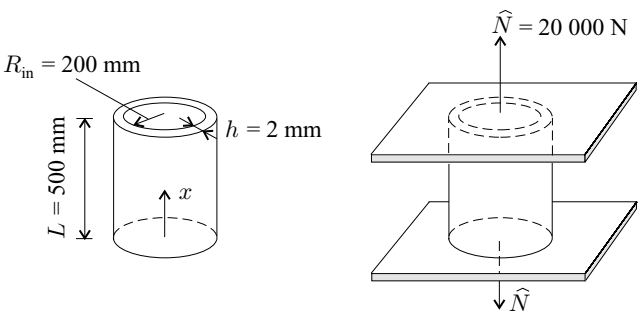

Figure 8.14: The cylinder in Example 8.1.

Solution. The radius of the reference surface, chosen as the midsurface, is

$$R = R_{\text{in}} + h/2 = 0.201 \text{ m}, \tag{8.43}$$

where h is the wall thickness ($h = 0.002$ m).

The axial load is $\widehat{N} = 20\,000$ N, and the torque $\widehat{T}$ is zero. The constants D_1 and D_2 are (Eqs. 8.32 and 8.34)

$$D_1 = N_x = \frac{\widehat{N}}{2\pi R} = 15\,836\,\frac{\text{N}}{\text{m}} \qquad D_2 = \frac{\widehat{T}}{2\pi R^2} = 0. \tag{8.44}$$

There is no radial load acting on the cylinder, and $p_{z0} = p_{z1} = 0$ (Eq. 8.13). The elements of the $[A]$, $[B]$, and $[D]$ matrices of the wall are given in Eq. (3.54). With the values in Eq. (3.54) the matrices in Table 8.2 (page 372) become

$$[a_1] = \begin{bmatrix} A_{22} - \frac{B_{22}}{R} & B_{12} \\ B_{12} - \frac{D_{12}}{R} & D_{11} \end{bmatrix} = \begin{bmatrix} 55.269 \times 10^6 & 16\,820 \\ 16\,806 & 64.842 \end{bmatrix} \tag{8.45}$$

$$[a_3] = \begin{bmatrix} A_{11} & A_{16} - \frac{2B_{16}}{R} \\ A_{16} + \frac{B_{16}}{R} & A_{66} - \frac{B_{66}}{R} - \frac{2D_{66}}{R^2} \end{bmatrix} = \begin{bmatrix} 194.52 & 34.62 \\ 34.88 & 42.66 \end{bmatrix} \times 10^6 \tag{8.46}$$

$$[a_2] = \begin{bmatrix} A_{12} - \frac{B_{12}}{R} & B_{11} \\ A_{26} - \frac{D_{26}}{R^2} & B_{16} + \frac{D_{16}}{R} \end{bmatrix} = \begin{bmatrix} 39.05 & -0.051\,61 \\ 34.79 & 0.017\,45 \end{bmatrix} \times 10^6 \tag{8.47}$$

$$[a_4] = \begin{bmatrix} A_{12} & A_{26} - \frac{2B_{26}}{R} \\ B_{11} & B_{16} - \frac{2D_{16}}{R} \end{bmatrix} = \begin{bmatrix} 39.46 & 34.62 \\ -0.051\,61 & 0.017\,28 \end{bmatrix} \times 10^6 \tag{8.48}$$

$$[H] = [a_1] - [a_4]\,[a_3]^{-1}\,[a_2] = \begin{bmatrix} 26.306 \times 10^6 & 7\,069 \\ 6\,987 & 31.755 \end{bmatrix} \tag{8.49}$$

$$\mathbf{g} = [a_4][a_3]^{-1} \begin{Bmatrix} D_1 \\ D_2 \end{Bmatrix} = \begin{Bmatrix} 1\,063 \\ -6.264 \end{Bmatrix}. \tag{8.50}$$

The constants f_1–f_5 are (Table 8.2, page 372)

$$\begin{aligned} f_1 &= H_{22} = 31.76 \qquad f_2 = -\frac{1}{R}\,(H_{21}{+}H_{12}) = -69\,931 \\ f_3 &= \frac{H_{11}}{R^2} = 651.13 \times 10^6 \qquad f_4 = p_{z0} - \frac{g_1}{R} = -5\,288 \\ f_5 &= p_{z1} = 0. \end{aligned} \tag{8.51}$$

With these f_i values the root of the characteristic polynomial is (Eq. 8.31)

$$\gamma = \sqrt{\frac{-f_2 + \sqrt{f_2^2 - 4\,f_1\,f_3}}{2\,f_1}} = 53.05 + 41.40\,i. \tag{8.52}$$

The parameters λ and β are

$$\lambda = \text{Re}(\gamma) = 53.05 \qquad \beta = \text{Im}(\gamma) = 41.40. \tag{8.53}$$

The expressions in Table 8.3 (page 374) give

$$\begin{aligned} Y_{13} &= -0.8258 \times 10^{-12} & Y_{14} &= 2.9021 \times 10^{-12} \\ Y_{23} &= 76.319 \times 10^{-12} & Y_{24} &= 188.15 \times 10^{-12} \\ Y_{31} &= -0.8258 \times 10^{-12} & Y_{32} &= 2.9021 \times 10^{-12} \\ Y_{41} &= -76.319 \times 10^{-12} & Y_{42} &= -188.15 \times 10^{-12}. \end{aligned} \tag{8.54}$$

By substituting the preceding values of f_i and Y_{ij} into Eq. (8.36), we obtain

$$\begin{bmatrix} 1 & 0 & Y_{13} & Y_{14} \\ -\lambda & \beta & Y_{23} & Y_{24} \\ Y_{31} & Y_{32} & 1 & 0 \\ Y_{41} & Y_{42} & \lambda & \beta \end{bmatrix} \begin{Bmatrix} C_1 \\ C_2 \\ C_3 \\ C_4 \end{Bmatrix} = \begin{Bmatrix} 8.121 \\ 0 \\ 8.121 \\ 0 \end{Bmatrix} \times 10^{-6}. \tag{8.55}$$

Solution of this set of equations gives the constants

$$\begin{aligned} C_1 &= 8.121 \times 10^{-6} & C_2 &= 10.41 \times 10^{-6} \\ C_3 &= 8.121 \times 10^{-6} & C_4 &= 10.41 \times 10^{-6}. \end{aligned} \tag{8.56}$$

The radial displacement is (Eq. 8.30)

$$\begin{aligned} w^{\mathrm{o}} = &\left\{ e^{-\lambda x}[C_1 \cos(\beta x) + C_2 \sin(\beta x)] \right. \\ &\left. + e^{-\lambda(L-x)}[C_3 \cos(\beta(L-x)) + C_4 \sin(\beta(L-x))] \right\} \\ &+ \left[\frac{1}{f_3}(f_4 + x f_5) \right]. \end{aligned} \tag{8.57}$$

With the rigid-body motions neglected, the axial and circumferential displacements are (Eq. 8.37)

$$\begin{Bmatrix} u^{\mathrm{o}} \\ v^{\mathrm{o}} \end{Bmatrix} = -[a_3]^{-1}[a_2] \begin{Bmatrix} \frac{\int w^{\mathrm{o}} dx}{R} \\ -\frac{dw^{\mathrm{o}}}{dx} \end{Bmatrix} + x[a_3]^{-1} \begin{Bmatrix} D_1 \\ D_2 \end{Bmatrix}, \tag{8.58}$$

where $\int w^{\mathrm{o}} dx$ and dw^{o}/dx are calculated by the expressions given in Table 8.4 (page 375).

The axial, circumferential, and radial displacements are calculated by Eqs. (8.57) and (8.58) together with the constants λ, β, C_1–C_4, f_4, f_5 given in Eqs. (8.51), (8.53), and (8.56). The results are plotted in Figure 8.15. The length of the boundary layer is (page 377) $L_{\mathrm{B}} = 4/\lambda = 0.0754$ m.

8.2.3 Temperature – Built-In Ends

We consider a cylinder with built-in ends on which the mechanical loads p_z, $\widehat{N}$, and $\widehat{T}$ act (Fig. 8.9) and that is subjected to a temperature change ΔT. This ΔT may vary in an arbitrary manner in the radial direction and linearly in the axial direction,

$$\Delta T(x, z) = \Delta T_z(z)(\Delta T_0 + x \Delta T_1), \tag{8.59}$$

where $\Delta T_z(z)$ is the temperature variation across the wall and ΔT_0, ΔT_1 are constants.

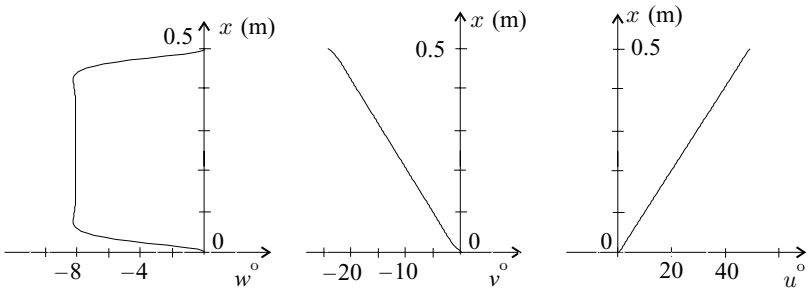

Figure 8.15: The radial w°, circumferential v°, and axial u° displacements of the cylinder wall in Example 8.1. The unit of the displacements is 10^{-6} m.

The equilibrium and strain–displacement relationships are given by Eqs. (8.14)–(8.20), and the relationships between the strains, curvatures, in-plane forces, and moments for plates are given by Eq. (4.251). The radial displacement can be calculated by the steps employed in Section 8.2.2. The resulting expression for w° is identical to Eq. (8.30), but now f_1, f_2, (which appear through λ), and f_3 are those given in Table 8.2 (page 372), and f_4 and f_5 are those in Table 8.6. The expressions for the axial and circumferential displacements become

$$\begin{Bmatrix} u^{\circ} \\ v^{\circ} \end{Bmatrix} = -[a_3]^{-1}[a_2] \begin{Bmatrix} \frac{\int w^{\circ} dx}{R} \\ -\frac{dw^{\circ}}{dx} \end{Bmatrix} + [a_3]^{-1} \left(x \begin{Bmatrix} D_1 \\ D_2 \end{Bmatrix} + \mathbf{b_T} \left(x \Delta T_0 + \frac{x^2}{2} \Delta T_1 \right) \right). \tag{8.60}$$

The vector $\mathbf{b_T}$ is defined in Table 8.6. Once the displacements are known, all other parameters of interest can be calculated. The strains are calculated by Eqs. (8.19) and (8.20), the forces and moments (per unit length) by Eq. (4.251).

8.3 Springback

When an unrestrained isotropic shell is heated to a uniform temperature, its size changes but not its shape. When a laminated shell is heated uniformly, both its size and shape change. This difference in the behavior of isotropic and laminated shells is illustrated in the next section for a cylindrical shell segment.[7]

8.3.1 Springback of Cylindrical Shells

To describe the springback phenomenon we examine a cylindrical shell segment whose temperature is changed uniformly by ΔT_0 (Fig. 8.16). Because of this temperature change the arclengths L_1 and L_2, the thickness h, and the subtended angle γ change to L_1', L_2', h', and γ'. The springback is defined as the change in

[7] N. Zahlan and J. M. O'Neill, Design and Fabrication of Composite Components; the Spring-Forward Phenomenon. *Composites*, Vol. 20, 77–81, 1989.

Table 8.6. The parameters required in Eq. (8.60)

$f_4 = p_{z0} - \frac{g_1}{R} - \Delta T_0 \frac{h_1}{R} \quad f_5 = p_{z1} - \Delta T_1 \frac{h_1}{R}$,

where

$\boldsymbol{h} = \begin{Bmatrix} h_1 \\ h_2 \end{Bmatrix} = [a_4][a_3]^{-1}\mathbf{b_T} - \mathbf{c_T}$, and $[a_3]$, $[a_4]$, g_1 are given in Table 8.2.

$$\mathbf{b_T} = \begin{bmatrix} A_{11} & A_{12} & A_{16} & B_{11} & B_{12} & B_{16} \\ A_{16} + \frac{B_{16}}{R} & A_{26} + \frac{B_{26}}{R} & A_{66} + \frac{B_{66}}{R} & B_{16} + \frac{D_{16}}{R} & B_{26} + \frac{D_{26}}{R} & B_{66} + \frac{D_{66}}{R} \end{bmatrix} \boldsymbol{\Omega}$$

$$\mathbf{c_T} = \begin{bmatrix} A_{12} & A_{22} & A_{26} & B_{12} & B_{22} & B_{26} \\ B_{11} & B_{12} & B_{16} & D_{11} & D_{12} & D_{16} \end{bmatrix} \boldsymbol{\Omega}$$

$\boldsymbol{\Omega}$ is the vector of hygrothermal strains caused by $\Delta T_z(z)$ defined by Eq. (4.250)

$\boldsymbol{\Omega} = \left\{ \epsilon_x^{\mathrm{o,ht}} \quad \epsilon_y^{\mathrm{o,ht}} \quad \gamma_{xy}^{\mathrm{o,ht}} \quad \kappa_x^{\mathrm{ht}} \quad \kappa_y^{\mathrm{ht}} \quad \kappa_{xy}^{\mathrm{ht}} \right\}^T$

the angle during heating or cooling as follows:

$$\text{springback} = \frac{\gamma' - \gamma}{\gamma}. \tag{8.61}$$

The angle γ is related to the arclengths and the thickness by (Fig. 8.16, left)

$$\gamma = \frac{L_1 - L_2}{h}. \tag{8.62}$$

Similarly, γ' is

$$\gamma' = \frac{L_1' - L_2'}{h'}. \tag{8.63}$$

When the segment is made of a single layer, the thermal strain ϵ^{ht} is $\widetilde{\alpha}\Delta T$. Thus, after deformation, the arclengths of the top and bottom surfaces and the thickness are (Fig. 8.16, right)

$$L_1' = L_1 + \widetilde{\alpha}_y \Delta T_0 L_1 \qquad L_2' = L_2 + \widetilde{\alpha}_y \Delta T_0 L_2 \qquad h' = h + \widetilde{\alpha}_z \Delta T_0 h, \tag{8.64}$$

where $\widetilde{\alpha}_y$ and $\widetilde{\alpha}_z$ are the thermal expansion coefficients in the y and z directions, respectively. Substitution of Eqs. (8.62)–(8.64) into Eq. (8.61) gives the springback

$$\text{springback} = \frac{(\widetilde{\alpha}_y - \widetilde{\alpha}_z)\,\Delta T_0}{1 + \widetilde{\alpha}_z \Delta T_0}. \tag{8.65}$$

When heated, an isotropic material (for which $\widetilde{\alpha}_y = \widetilde{\alpha}_z$) expands equally in every direction. Thus, when heated uniformly, the springback of an isotropic

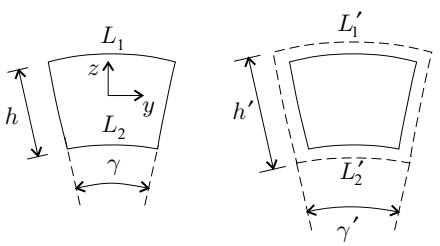

Figure 8.16: Cylindrical shell segment. Undeformed element (left) and the element deformed due to a uniform change in temperature (right).

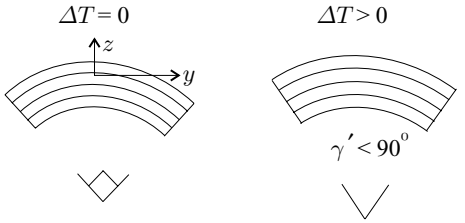

Figure 8.17: Springback of a composite segment made of unidirectional fiber-reinforced matrix.

cylindrical segment is zero; the size of the segment changes but not its shape. On the other hand, in a composite material the thermal expansion coefficient of the matrix differs from that of the fibers. Thus, for example, a heated segment made of identical layers containing fibers in the circumferential direction (Fig. 8.17) expands more in the z direction than in the y direction ($\widetilde{\alpha}_y < \widetilde{\alpha}_z$). In this case the springback is nonzero and the segment bends. (A similar argument holds when the segment is cooled.)

The thermal strains are generally small compared with unity, and the springback may be approximated by

$$\text{springback} = (\widetilde{\alpha}_y - \widetilde{\alpha}_z)\,\Delta T_0 = \epsilon_y^{\text{ht}} - \epsilon_z^{\text{ht}}. \tag{8.66}$$

This expression, derived for a single layer, may also be used for laminated composites with appropriate values of ϵ_y^{ht} and ϵ_z^{ht}. For a laminated composite the average hygrothermal strain perpendicular to the surface is approximated by

$$\epsilon_z^{\text{ht}} = \frac{h' - h}{h} = \frac{\Delta h}{h}, \tag{8.67}$$

where the change in thickness Δh is given by Eq. (4.287). The circumferential hygrothermal strain is approximated by the in-plane hygrothermal strain of a flat laminate given in Eq. (4.250)

$$\epsilon_y^{\text{ht}} = \epsilon_y^{\text{o,ht}} = \{\alpha_{12} \quad \alpha_{22} \quad \alpha_{26} \quad \beta_{12} \quad \beta_{22} \quad \beta_{26}\} \begin{Bmatrix} N_x^{\text{ht}} \\ N_y^{\text{ht}} \\ N_{xy}^{\text{ht}} \\ M_x^{\text{ht}} \\ M_y^{\text{ht}} \\ M_{xy}^{\text{ht}} \end{Bmatrix}. \tag{8.68}$$

When the layup is symmetrical, the springback of a cylindrical segment is given by Eq. (8.66) with the strains in Eqs. (8.67) and (8.68). When the layup is unsymmetrical, an additional term must be included in the springback. This term is arrived at by observing that a flat plate with symmetrical layup does not bend when the plate's temperature is changed uniformly. On the other hand a flat plate with unsymmetrical layup bends when the temperature of the plate is changed uniformly. The change in curvature is κ_y^{ht}. Hence, the total springback of a segment with unsymmetrical layup is

$$\text{springback} = R\kappa_y^{\text{ht}} + \left(\epsilon_y^{\text{o,ht}} - \epsilon_z^{\text{ht}}\right) \qquad \begin{matrix} \text{unsymmetrical} \\ \text{segment.} \end{matrix} \tag{8.69}$$

where κ_y^{ht} is approximated by the hygrothermal curvature of a flat laminate given

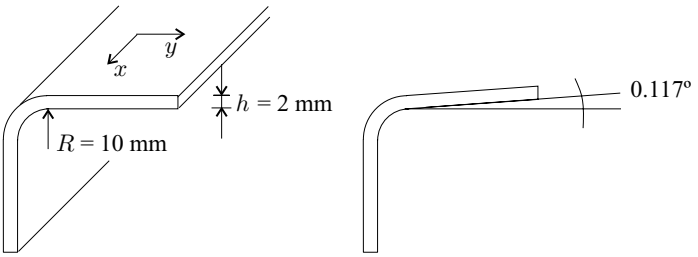

Figure 8.18: L-shaped stiffener in Example 8.2.

by Eq. (4.250) as follows:

$$\kappa_y^{\text{ht}} = \{\beta_{12} \quad \beta_{22} \quad \beta_{26} \quad \delta_{12} \quad \delta_{22} \quad \delta_{26}\} \begin{Bmatrix} N_x^{\text{ht}} \\ N_y^{\text{ht}} \\ N_{xy}^{\text{ht}} \\ M_x^{\text{ht}} \\ M_y^{\text{ht}} \\ M_{xy}^{\text{ht}} \end{Bmatrix}. \tag{8.70}$$

When a cylindrical shell or circular cylinder is analyzed, this springback effect must be included in the hygrothermal force–strain relationship of laminated plates. This is accomplished by making the following replacement in Eq. (4.251):

$$\begin{array}{cc} \text{Laminated plate} & \text{Cylindrical shell} \\ \text{(Eq. 4.251)} & \\ \kappa_y^{\text{ht}} & \Longrightarrow \kappa_y^{\text{ht}} + \dfrac{1}{R}\left(\epsilon_y^{\text{o,ht}} - \epsilon_z^{\text{ht}}\right). \end{array} \tag{8.71}$$

8.2 Example. *An L-shaped stiffener (Fig. 8.18) is made of graphite epoxy unidirectional plies. The material properties are listed in Table 3.6 (page 81). The layup is* $[45_6/0_4]_s$. *The* 0*-degree plies are along the length of the stiffener. The thickness of the wall is* $h = 0.002$ *m. The temperature is raised by* $80\ ^\circ$*C. Determine the new shape of the stiffener.*

Solution. The springback is (Eqs. 8.66 and 8.67)

$$\text{springback} = \epsilon_y^{\text{ht}} - \frac{\Delta h}{h} = 1.653 \times 10^{-3} - \frac{5.899 \times 10^{-6}}{2 \times 10^{-3}} = -1.297 \times 10^{-3}, \tag{8.72}$$

where h is the thickness of the wall ($h = 0.002$ m), Δh is the change in thickness due to the temperature change ($\Delta h = 5.899 \times 10^{-6}$ m, Eq. 4.295), and ϵ_y^{ht} is the strain in the circumferential direction ($\epsilon_y^{\text{ht}} = 1.653 \times 10^{-3}$, Eq. 4.273).

The change in the angle of the 90-degree stiffener is (Eq. 8.61)

$$\gamma' - \gamma = \text{springback} \times 90^\circ = -0.117^\circ. \tag{8.73}$$

This is illustrated in Figure 8.18, right. The layup of the stiffener is unbalanced and, therefore, the stiffener will also twist.

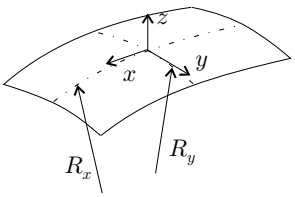

Figure 8.19: Radii of curvatures R_x, R_y of a shell.

8.3.2 Doubly Curved Shells

We generalize the preceding result (Eq. 8.71) and extend it to doubly curved shells with radii of curvatures R_x, R_y in the x–z and y–z planes (Fig. 8.19). In this case, the following replacements must be made in the laminated plate hygrothermal stress–strain relationships (Eq. 4.251):

$$\begin{array}{ll} \text{Laminated plate} & \text{Doubly curved shell} \\ \kappa_x^{\mathrm{ht}} \Longrightarrow & \kappa_x^{\mathrm{ht}} + \dfrac{1}{R_x}\left(\epsilon_x^{\mathrm{o,ht}} - \epsilon_z^{\mathrm{ht}}\right) \\ \kappa_y^{\mathrm{ht}} \Longrightarrow & \kappa_y^{\mathrm{ht}} + \dfrac{1}{R_y}\left(\epsilon_y^{\mathrm{o,ht}} - \epsilon_z^{\mathrm{ht}}\right). \end{array} \tag{8.74}$$

8.4 Buckling of Shells

We consider a composite shell subjected simultaneously to surface loads on the wall and compressive and shear loads at the edges (Fig. 8.20). When this load set is increased beyond its critical limit, the shell buckles either globally or locally away from the edges. In general, local buckling precedes global buckling. In the following we treat local buckling of laminated composite shells.

We consider a small element away from the edges. The membrane forces acting on this element are (Fig. 8.20, right)

$$N_x = -\lambda N_{x0} \qquad N_y = -\lambda N_{y0} \qquad N_{xy} = -\lambda N_{xy0}, \tag{8.75}$$

where λ is the load parameter. We are interested in the value of λ (denoted by λ_{cr}) at which the shell locally buckles. An analysis describing the local buckling of shells was presented by Kollár.[8] In this analysis the buckling load is derived by representing the short waves arising at the location of the buckling by trigonometric functions. The derivation is long and involved and is not given here. We only quote the results for shells that are shallow[9] in the region where the local buckling occurs, and in this region the shell has constant curvatures (R_x = constant, R_y = constant, and R_{xy} = constant). The reference surface is designated by the function $f(x, y)$ (Table 8.7) and the radii of curvatures are $1/R_x = -\partial^2 f/\partial x^2$,

[8] L. P. Kollár, Buckling of Generally Anisotropic Shallow Sandwich Shells. *Journal of Reinforced Plastics and Composites,* Vol. 9, 549–568, 1990.

[9] W. Flügge, *Stresses in Shells.* 2nd edition. Springer, Berlin, 1973, p. 414.

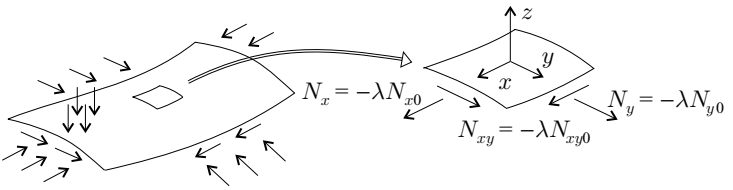

Figure 8.20: Surface and edge loads on a shell and the membrane forces.

$1/R_y = -\partial^2 f/\partial y^2, 1/R_{xy} = -2\partial^2 f/\partial x \partial y$. For such shells, the resulting equation is

$$\left(\begin{bmatrix} O & L \\ L & O \end{bmatrix} \begin{bmatrix} M_o & M_n \\ M_n & M_o \end{bmatrix} \begin{bmatrix} O & L \\ L & O \end{bmatrix}^T - \lambda \begin{bmatrix} \Phi_1[J] & \Phi_2[J] \\ \Phi_2[J] & \Phi_1[J] \end{bmatrix} \right) \begin{Bmatrix} u_1 \\ v_1 \\ w_1 \\ u_2 \\ v_2 \\ w_2 \end{Bmatrix} = 0, \quad (8.76)$$

where u_1, v_1, u_2, v_2 are the in-plane and w_1, w_2 are the out-of-plane amplitudes of the buckling waves. The matrices $[O]$, $[L]$, $[J]$ and the parameters Φ_1, Φ_2 (given in Table 8.8) depend on four constants α, β, c_1, c_2, which characterize the wave pattern of the buckled shape (Fig. 8.21).

Table 8.7. Curvatures of typical shells

	$f(x, y)$	R_x	R_y	R_{xy}
cylinder 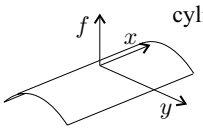	$f = -C_1 y^2$	0	$\frac{1}{2C_1}$	0
elliptical paraboloid 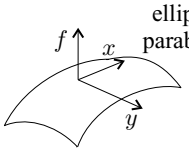	$f = -C_1 y^2 - C_2 x^2$	$\frac{1}{2C_2}$	$\frac{1}{2C_1}$	0
hyperbolic paraboloid 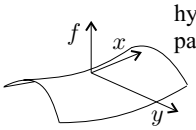	$f = -C_1 y^2 + C_2 x^2$	$-\frac{1}{2C_2}$	$\frac{1}{2C_1}$	0
hyperbolic paraboloid 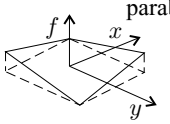	$f = -C_1 xy$	0	0	$\frac{1}{2C_1}$

Table 8.8. The parameters required in Eqs. (8.76) and (8.89). For a cylinder $1/R_x = 1/R_{xy} = 0$ and $R_y = R$

$$[O] = \begin{bmatrix} -\alpha & 0 & \beta & 0 & 0 & 0 \\ 0 & -\beta & \alpha & 0 & 0 & 0 \\ \frac{1}{R_x} & \frac{1}{R_y} & 0 & \alpha^2+\beta^2c_2^2 & \beta^2+\alpha^2c_1^2 & -2\alpha\beta\,(1+c_1c_2) \end{bmatrix}$$

$$[L] = \begin{bmatrix} \beta c_2 & 0 & -\alpha c_1 & 0 & 0 & 0 \\ 0 & \alpha c_1 & -\beta c_2 & 0 & 0 & 0 \\ 0 & 0 & \frac{1}{R_{xy}} & -2\alpha\beta c_2 & -2\alpha\beta c_1 & 2(c_1\alpha^2+c_2\beta^2) \end{bmatrix}$$

$$[M_o] = \begin{bmatrix} A_{11} & A_{12} & 0 & B_{11} & B_{12} & 0 \\ A_{12} & A_{22} & 0 & B_{12} & B_{22} & 0 \\ 0 & 0 & A_{66} & 0 & 0 & B_{66} \\ B_{11} & B_{12} & 0 & D_{11} & D_{12} & 0 \\ B_{12} & B_{22} & 0 & D_{12} & D_{22} & 0 \\ 0 & 0 & B_{66} & 0 & 0 & D_{66} \end{bmatrix} \qquad [M_n] = \begin{bmatrix} A & B \\ B & D \end{bmatrix} - [M_o]$$

$$[J] = \begin{bmatrix} 0 & 0 & 0 \\ 0 & 0 & 0 \\ 0 & 0 & 1 \end{bmatrix}$$

$$\Phi_1 = N_{x0}\left(\alpha^2+\beta^2c_2^2\right) + N_{xy0}2\left(\alpha^2c_1+\beta^2c_2^2\right) + N_{y0}\left(\alpha^2c_1+\beta^2\right)$$

$$\Phi_2 = -2\alpha\beta(N_{x0}c_2 + N_{xy0}(1+c_1c_2) + N_{y0}c_1)$$

The directions of the lines passing through the maxima of the left and right propagating waves are (Fig 8.22)

$$\tan\vartheta_1 = \frac{\alpha+\beta c_2}{\beta+\alpha c_1} \qquad \tan\vartheta_2 = \frac{\alpha-\beta c_2}{\beta-\alpha c_1}. \tag{8.77}$$

The eigenvalues λ_{cr} of Eq. (8.76) are the critical load parameters, which are to be calculated for different values of the constants α, β, c_1, c_2. The lowest value of λ_{cr} resulting from these calculations is the value of interest. In principle, the values of these constants can not be selected arbitrarily, but must be chosen such that the corresponding displacements satisfy the boundary conditions. For short wavelengths, which is the case considered here, the edges do not affect the waves significantly and, hence, the buckling load. Therefore, as an approximation, arbitrary values of α, β, c_1, c_2 may be chosen for calculating λ_{cr}.

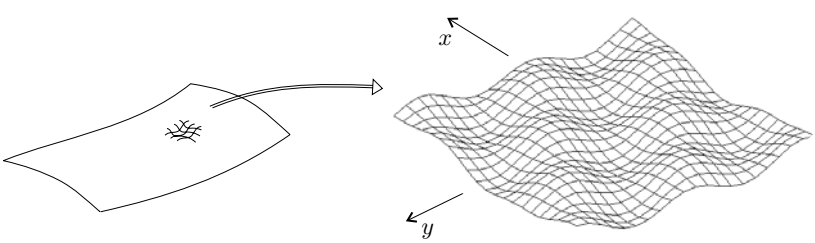

Figure 8.21: Illustration of the buckling pattern at local buckling of a shell.

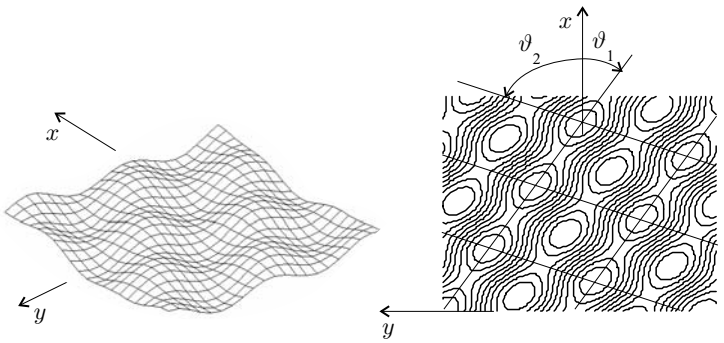

Figure 8.22: The local buckling pattern and the corresponding contour plot.

Once the constants α, β, c_1, and c_2 are known, the deflection perpendicular to the reference surface of the shell is calculated by

$$w_{\mathrm{B}}^{\mathrm{o}} = w_1 \sin\left(\alpha(x + c_1 y)\right) \sin\left(\beta(y + c_2 x)\right) + \; w_2 \sin\left(\alpha(x + c_1 y)\right) \cos\left(\beta(y + c_2 x)\right). \tag{8.78}$$

8.4.1 Buckling of Cylinders

The buckling analysis presented earlier in this section for thin shallow shells may be applied to the buckling of thin cylinders by setting the radius R equal to the radius R_y of the shell ($R = R_y$), and R_x and R_{xy} to infinity ($1/R_x = 1/R_{xy} = 0$).

8.3 Example. *An $L = 1$-m-long cylinder (inner radius $R_{in} = 0.2$ m) is made of graphite epoxy unidirectional plies. The material properties are given in Table 3.6 (page 81). The layup is $[-30_4/15_4/0_2]_{\mathrm{s}}$. The 0-degree plies are parallel to the cylinder axis. The thickness of the wall is $h = 0.002$ m (Fig. 8.23). An axial load is applied to the cylinder. Calculate the load that causes local buckling.*

Solution. For this cylinder we have

$$\begin{aligned} &R = R_y = R_{\mathrm{in}} + h/2 = 0.201 \text{ m} \qquad 1/R_x = 1/R_{xy} = 0 \\ &N_{y0} = N_{xy0} = 0. \end{aligned} \tag{8.79}$$

For N_{x0} we arbitrarily select the value $N_{x0} = 1$. With this value and with the values in Eq. (8.79), the matrices $[O]$ and $[L]$ and the parameters Φ_1, Φ_2 are

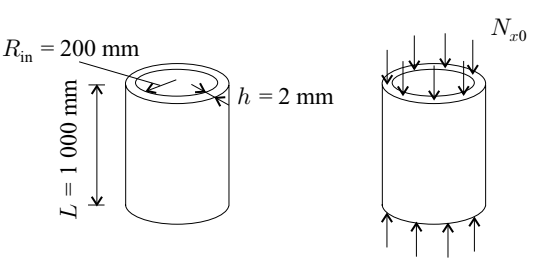

Figure 8.23: The cylinder in Example 8.3.

(Table 8.8, page 386)

$$[O] = \begin{bmatrix} -\alpha & 0 & \beta & 0 & 0 & 0 \\ 0 & -\beta & \alpha & 0 & 0 & 0 \\ 0 & 4.975 & 0 & \alpha^2 + \beta^2 c_2^2 & \beta^2 + \alpha^2 c_1^2 & -2\alpha\beta\,(1 + c_1 c_2) \end{bmatrix} \tag{8.80}$$

$$[L] = \begin{bmatrix} \beta c_2 & 0 & -\alpha c_1 & 0 & 0 & 0 \\ 0 & \alpha c_1 & -\beta c_2 & 0 & 0 & 0 \\ 0 & 0 & 0 & -2\alpha\beta c_2 & -2\alpha\beta c_1 & 2(c_1\alpha^2 + c_2\beta^2) \end{bmatrix} \tag{8.81}$$

$$\Phi_1 = \alpha^2 + \beta^2 c_2^2 \tag{8.82}$$

$$\Phi_2 = -2\alpha\beta c_2. \tag{8.83}$$

The matrices $[M_o]$, $[M_n]$ and $[J]$ (Table 8.8, page 386), with the elements of the $[A]$ and $[D]$ matrices given in Table 3.7 (page 84), are

$$[M_o] = \begin{bmatrix} 235.54 \times 10^6 & 32.74 \times 10^6 & 0 & 0 & 0 & 0 \\ 32.74 \times 10^6 & 27.79 \times 10^6 & 0 & 0 & 0 & 0 \\ 0 & 0 & 36.01 \times 10^6 & 0 & 0 & 0 \\ 0 & 0 & 0 & 65.42 & 16.29 & 0 \\ 0 & 0 & 0 & 16.29 & 11.60 & 0 \\ 0 & 0 & 0 & 0 & 0 & 17.39 \end{bmatrix}$$

$$[M_n] = \begin{bmatrix} 0 & 0 & -10.19 \times 10^6 & 0 & 0 & 0 \\ 0 & 0 & -10.19 \times 10^6 & 0 & 0 & 0 \\ -10.19 \times 10^6 & -10.19 \times 10^6 & 0 & 0 & 0 & 0 \\ 0 & 0 & 0 & 0 & 0 & -18.93 \\ 0 & 0 & 0 & 0 & 0 & -7.74 \\ 0 & 0 & 0 & -18.93 & -7.74 & 0 \end{bmatrix}$$

$$[J] = \begin{bmatrix} 0 & 0 & 0 \\ 0 & 0 & 0 \\ 0 & 0 & 1 \end{bmatrix}.$$

To find λ_{cr}, we refer to Eq. (8.76):

$$\left(\underbrace{\begin{bmatrix} O & L \\ L & O \end{bmatrix} \begin{bmatrix} M_o & M_n \\ M_n & M_o \end{bmatrix} \begin{bmatrix} O & L \\ L & O \end{bmatrix}^T}_{[G]} - \lambda \begin{bmatrix} \Phi_1[J] & \Phi_2[J] \\ \Phi_2[J] & \Phi_1[J] \end{bmatrix} \right) \begin{Bmatrix} u_1 \\ v_1 \\ w_1 \\ u_2 \\ v_2 \\ w_2 \end{Bmatrix} = 0. \tag{8.84}$$

To obtain λ and the displacements we assume different values of the parameters α, β, c_1, c_2. For example, we set $\alpha = 40$, $\beta = 40$, $c_1 = 0$, $c_2 = 0$. With these values

Eq. (8.84) becomes

$$\left([G] - \lambda \begin{bmatrix} 0 & & & & & \\ & 0 & & & & \\ & & 1\,600 & & & \\ & & & 0 & & \\ & & & & 0 & \\ & & & & & 1\,600 \end{bmatrix} \right) \begin{Bmatrix} u_1 \\ v_1 \\ w_1 \\ u_2 \\ v_2 \\ w_2 \end{Bmatrix} = 0, \tag{8.85}$$

where

$$[G] = \begin{bmatrix} 434.49 & 109.99 & -6.5145 & 32.601 & 32.601 & -2.0274 \\ 109.99 & 102.09 & -5.5311 & 32.601 & 32.601 & -2.0274 \\ -6.5145 & -5.5311 & 1.1466 & -2.0274 & -2.0274 & 0.27312 \\ 32.601 & 32.601 & -2.0274 & 434.49 & 109.99 & -6.5145 \\ 32.601 & 32.601 & -2.0274 & 109.99 & 102.09 & -5.5311 \\ -2.0274 & -2.0274 & 0.27312 & -6.5145 & -5.5311 & 1.1466 \end{bmatrix} \times 10^9.$$

Solution of Eq. (8.85) yields

$$\lambda_{\text{cr}} = 434\,810 \qquad \text{for} \quad \begin{array}{l} \alpha = 40 \\ \beta = 40 \\ c_1 = 0 \\ c_2 = 0\,. \end{array}$$

We are interested in the lowest value of λ_{cr}. To find this value we repeat the calculation for different sets of α, β, c_1, c_2 values. The lowest value of λ_{cr} corresponds to $\alpha = 37.5, \beta = 16.4, c_1 = 0.152, c_2 = 1.3$. For these α, β, c_1, c_2 values the results are

$$\lambda_{\text{cr}} = 345\,568 \qquad \text{for} \quad \begin{array}{l} \alpha = 37.5 \\ \beta = 16.4 \\ c_1 = 0.152 \\ c_2 = 1.3\,. \end{array}$$

The buckling load is

$$N_{x,\text{cr}} = \lambda_{\text{cr}} N_{x0} = 345\,568 \text{ N/m} = 346 \text{ kN/m}. \tag{8.86}$$

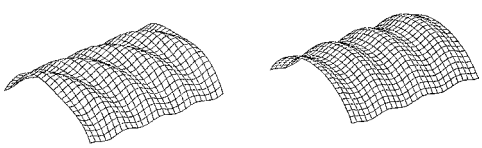

Figure 8.24: The buckled shape of the anisotropic cylinder in Example 8.3 (left) and the buckled shape on the assumption that the cylinder is orthotropic (right).

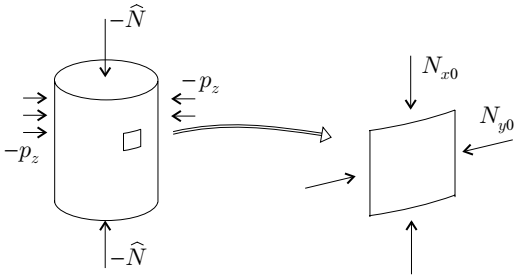

Figure 8.25: Cylinder subjected to axial load and pressure.

The directions of the lines passing through the maxima of the left and right propagating waves are (Eq. 8.77)

$$\vartheta_1 = \arctan \frac{\alpha + \beta c_2}{\beta + \alpha c_1} = 69.4^\circ \qquad \vartheta_2 = \arctan \frac{\alpha - \beta c_2}{\beta - \alpha c_1} = 56.5^\circ. \tag{8.87}$$

Solution of Eq. (8.84) also gives the amplitudes (see Eq. 8.78) of the displacements. For $\alpha = 37.5, \beta = 16.4, c_1 = 0.152$, and $c_2 = 1.3$ the amplitudes of the radial displacements are

$$w_1 = -0.707\ 06 \qquad w_2 = 0.707\ 06. \tag{8.88}$$

The buckled shape (Eq. 8.78) determined by these amplitudes is shown in Figure 8.24, left.

In the following we consider cylinders subjected to an axial load $-\widehat{N}$ and to a radial pressure $-p_z$ (Fig. 8.25). The membrane forces are $N_{x0} = -\widehat{N}/2\pi R$ and $N_{y0} = -p_z R$.

Orthotropic wall. The layup of the wall of the cylinder is orthotropic, and one of the directions of orthotropy coincides with x. For this case we assume that the cylinder buckles in a checkerboard pattern (Figs. 8.26 and 8.27). For this checkerboard pattern $\vartheta = \vartheta_1 = \vartheta_2 = \arctan \frac{l_x}{l_y}$, and from Eq. (8.77) we have that $c_1 = c_2 = 0$. Equation (8.76) now reduces to

$$([O][M_o][O]^T - \lambda \Phi_1 [J]) \begin{Bmatrix} u_1 \\ v_1 \\ w_1 \end{Bmatrix} = 0, \tag{8.89}$$

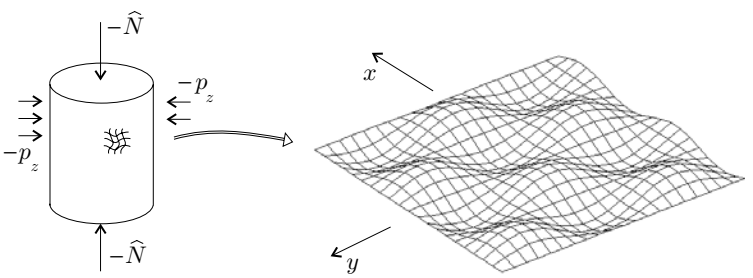

Figure 8.26: Illustration of the checkerboard buckling pattern at local buckling of an orthotropic cylinder subjected to axial load and uniform pressure.

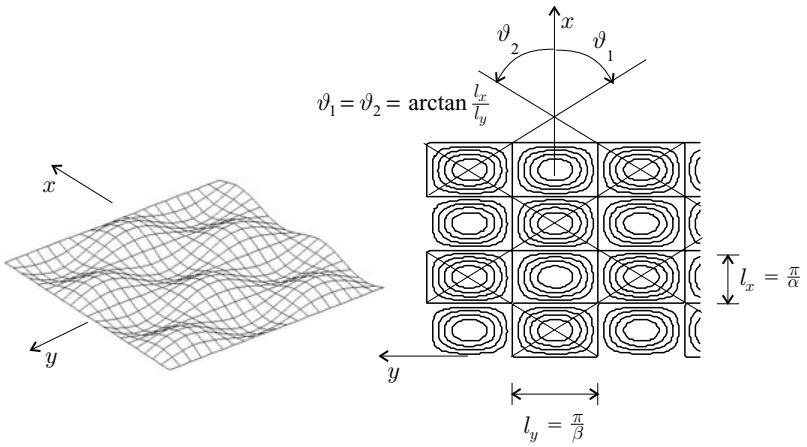

Figure 8.27: The local checkerboard buckling pattern and the corresponding contour plot of an orthotropic cylinder subjected to axial load and uniform pressure.

where the matrix $[O]$ and the parameter Φ_1, given in Table 8.8, are evaluated with $c_1 = c_2 = 0$. The eigenvalues of this equation are

$$\lambda_{cr} = \frac{1}{N_{x0}\alpha^2 + N_{y0}\beta^2} \frac{\begin{vmatrix} F_{11} & F_{12} & F_{13} \\ F_{12} & F_{22} & F_{23} \\ F_{13} & F_{23} & F_{33} \end{vmatrix}}{\begin{vmatrix} F_{11} & F_{12} \\ F_{12} & F_{22} \end{vmatrix}}, \tag{8.90}$$

where $||$ denotes the determinant. The elements F_{ij} $(i, j = 1, 2, 3)$ are given in Table 8.9 (page 392). The critical load parameter λ_{cr} (Eq. 8.90) must be calculated for different values of α and β. The lowest λ_{cr} is the value of interest.

Orthotropic and symmetrical wall. When the wall's layup is orthotropic and symmetrical ($B_{ij} = 0$), Eq. (8.90) simplifies to[10]

$$\lambda_{cr} = \frac{1}{N_{x0}\alpha^2 + N_{y0}\beta^2} \left\{ \left[\frac{\frac{\alpha^4}{R^2}\left(1 - \frac{A_{12}^2}{A_{11}A_{22}}\right)}{\frac{\alpha^4}{A_{22}} + \alpha^2\beta^2\left(\frac{1}{A_{66}} - \frac{A_{12}(A_{12}+2A_{66})}{A_{11}A_{22}A_{66}}\right) + \frac{\beta^4}{A_{11}}} \right] \right.$$
$$\left. + D_{11}\alpha^4 + 2\left(D_{12} + 2D_{66}\right)\beta^2\alpha^2 + D_{22}\beta^4 \right\}, \tag{8.91}$$

where λ_{cr} (Eq. 8.91) must be calculated for different values of α and β. The lowest λ_{cr} is the value of interest. When $R = \infty$, the term in parentheses is zero, and the expression above reduces to that for flat plates (Eq. 4.121).

8.4 Example. *An $L = 1$-m-long cylinder (inner radius $R_{in} = 0.2$ m) is made of graphite epoxy unidirectional plies (Fig. 8.28). The material properties are given in*

[10] R. M. Jones, Buckling of Circular Cylindrical Shells with Multiple Orthotropic Layers and Eccentric Stiffeners. *AIAA Journal,* Vol. 6, 2301–2305, 1968.

Table 8.9. The parameters required in Eqs. (8.90) and (8.96).

$$F_{11} = A_{11}\alpha^2 + A_{66}\beta^2 \qquad F_{12} = (A_{12} + A_{66})\,\alpha\beta$$
$$F_{13} = -A_{12}\tfrac{\alpha}{R} - B_{11}\alpha^3 - B_{12}\alpha\beta^2 - 2B_{66}\alpha\beta^2$$
$$F_{22} = A_{22}\beta^2 + A_{66}\alpha^2$$
$$F_{23} = -B_{22}\beta^3 - B_{12}\alpha^2\beta - 2B_{66}\alpha^2\beta - A_{22}\tfrac{\beta}{R}$$
$$F_{33} = D_{11}\alpha^4 + 2\,(D_{12} + 2D_{66})\,\beta^2\alpha^2 + D_{22}\beta^4 + \tfrac{1}{R}\left(A_{22}\tfrac{1}{R} + 2B_{22}\beta^2 + 2B_{12}\alpha^2\right)$$

Table 3.6 (page 81). The layup is $[-30_4/15_4/0_2]_s$. *The* 0*-degree plies are parallel to the cylinder axis. The thickness of the wall is* $h = 0.002$ *m. An axial load is applied to the cylinder. Calculate the buckling load that causes local buckling.*

Solution. The layup follows the 10-percent rule (page 89), and, accordingly, we may treat the cylinder as orthotropic. The layup is symmetrical and λ_{cr} is calculated by Eq. (8.91)

$$\lambda_{cr} = \frac{1}{N_{x0}\alpha^2 + N_{y0}\beta^2}\left\{\left[\frac{\frac{\alpha^4}{R^2}\left(1 - \frac{A_{12}^2}{A_{11}A_{22}}\right)}{\frac{\alpha^4}{A_{22}} + \alpha^2\beta^2\left(\frac{1}{A_{66}} - \frac{A_{12}(A_{12}+2A_{66})}{A_{11}A_{22}A_{66}}\right) + \frac{\beta^4}{A_{11}}}\right]\right.$$
$$\left. + D_{11}\alpha^4 + 2\,(D_{12} + 2D_{66})\,\beta^2\alpha^2 + D_{22}\beta^4\right\}. \tag{8.92}$$

For this cylinder we have

$$\begin{aligned} &R = R_y = R_{in} + h/2 = 0.201 \text{ m} \qquad 1/R_x = 1/R_{xy} = 0 \\ &N_{y0} = N_{xy0} = 0. \end{aligned} \tag{8.93}$$

For N_{x0} we arbitrarily select the value $N_{x0} = 1$.

With these values and with the elements of the $[A]$ and $[D]$ matrices in Table 3.7 (page 84), Eq. (8.92) becomes

$$\lambda_{cr} = \frac{1}{\alpha^2}\left\{\left[\frac{20.7\alpha^4}{(35.98\alpha^4 + 13.22\alpha^2\beta^2 + 4.246\beta^4)\,10^{-9}}\right]\right.$$
$$\left. + 65.42\alpha^4 + 102.1\beta^2\alpha^2 + 11.60\beta^4\right\}, \tag{8.94}$$

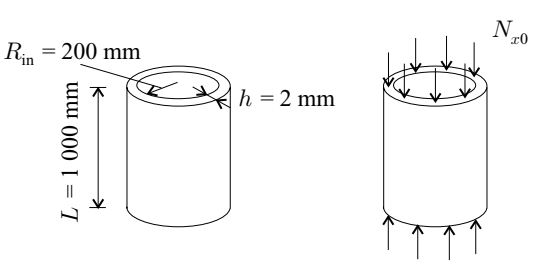

Figure 8.28: The cylinder in Example 8.4.

Table 8.10. The parameters in Eq. (8.96).

$$F_{14} = B_{11}\alpha^2 + B_{66}\beta^2 \qquad F_{15} = (B_{12} + B_{66})\,\alpha\beta$$
$$F_{24} = (B_{12} + B_{66})\,\alpha\beta \qquad F_{25} = B_{22}\beta^2 + B_{66}\alpha^2$$
$$F_{34} = -D_{11}\alpha^3 - (D_{12} + 2D_{66})\,\alpha\beta^2 - \tfrac{1}{R}B_{12}\alpha$$
$$F_{35} = -D_{22}\beta^3 - (D_{12} + 2D_{66})\,\alpha^2\beta - \tfrac{1}{R}B_{22}\beta$$
$$F_{44} = D_{11}\alpha^2 + D_{66}\beta^2 + \widetilde{S}_{11} \qquad F_{45} = (D_{12} + D_{66})\,\alpha\beta$$
$$F_{55} = D_{22}\beta^2 + D_{66}\alpha^2 + \widetilde{S}_{22}$$

where λ_{cr} is to be calculated for different of α and β values. We are interested in α and β that result in the lowest value of λ_{cr}. In this case, λ_{cr} is minimum for $\alpha = 54.5$ and $\beta \approx 0$ and has the value $\lambda_{\text{cr}} = 388$. Thus, the buckling load is

$$N_{x,\,\text{cr}} = \lambda_{\text{cr}} N_{x0} = 388 \text{ kN/m}. \tag{8.95}$$

We also calculated the buckled shape, which is axisymmetrical, as shown in Figure 8.24, right. The buckling load calculated with the assumption that the wall is orthotropic agrees within 12 percent with the result of the "exact" analysis ($N_{x,\text{cr}} = 346$ kN, Eq. 8.86).

Sandwich cylinder. When the cylinder's wall is of orthotropic sandwich construction (page 176), λ_{cr} is[11]

$$\lambda_{\text{cr}} = \frac{1}{N_{x0}\alpha^2 + N_{y0}\beta^2} \frac{\begin{vmatrix} F_{11} & F_{12} & F_{13} & F_{14} & F_{15} \\ F_{12} & F_{22} & F_{23} & F_{24} & F_{25} \\ F_{13} & F_{23} & F_{33} & F_{34} & F_{35} \\ F_{14} & F_{24} & F_{34} & F_{44} & F_{45} \\ F_{15} & F_{25} & F_{35} & F_{45} & F_{55} \end{vmatrix}}{\begin{vmatrix} F_{11} & F_{12} \\ F_{12} & F_{22} \end{vmatrix} \begin{vmatrix} F_{44} & F_{45} \\ F_{45} & F_{55} \end{vmatrix}}, \tag{8.96}$$

where the elements F_{ij} are given in a Tables 8.9 and 8.10 and λ_{cr} (Eq. 8.96) must be calculated for different values of α and β. The lowest resulting value of λ_{cr} is the value of interest. For $R = \infty$ this expression reduces to that for flat sandwich plates (Eq. 5.91).

When the cylinder wall is of isotropic or quasi-isotropic sandwich construction (page 176), Eq. (8.96) simplifies to

$$\lambda_{\text{cr}} = \frac{1}{N_{x0}\alpha^2 + N_{y0}\beta^2} \left\{ A^{\text{iso}}(1 - (\nu^{\text{iso}})^2) \frac{\left(\frac{\alpha^2}{R}\right)^2}{(\alpha^2 + \beta^2)^2} \right.$$
$$\left. + \left[\frac{1}{D^{\text{iso}}\,(\alpha^2 + \beta^2)^2} + \frac{1}{\widetilde{S}\,(\alpha^2 + \beta^2)} \right]^{-1} \right\}, \tag{8.97}$$

[11] L. P. Kollár, Buckling of Generally Anisotropic Shallow Sandwich Shells. *Journal of Reinforced Plastics and Composites,* Vol. 9, 549–568, 1990.

where ν^{iso}, A^{iso}, and D^{iso} are given in Table 5.2 (page 178) and $\widetilde{S}$ is given by Eq. (5.39). When the cylinder is subjected to axial compression only ($N_{y0} = 0$, see Eq. 8.11), the cylinder buckles axisymmetrically[12] ($\beta = 0$) and Eq. (8.97) becomes

$$\lambda_{\text{cr}} = \frac{1}{N_{x0}} \left[A^{\text{iso}}(1 - (\nu^{\text{iso}})^2) \frac{1}{R^2} \frac{1}{\alpha^2} + \left(\frac{1}{D^{\text{iso}} \alpha^2} + \frac{1}{\widetilde{S}} \right)^{-1} \right]. \tag{8.98}$$

The lowest value of λ_{cr} is obtained from the condition

$$\frac{\partial \lambda_{\text{cr}}}{\partial \alpha} = 0. \tag{8.99}$$

[12] I. Hegedűs, Buckling of Axially Compressed Cylindrical Sandwich Shells. *Acta Technica Hungarica*, Vol. 89, 377–387, 1979.